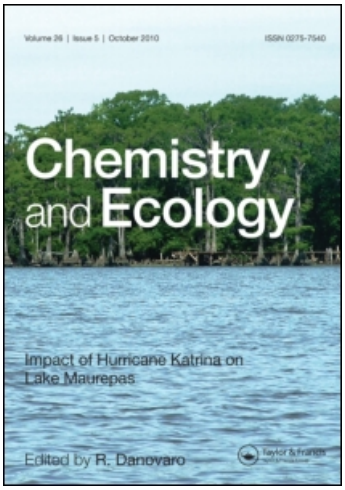


**Chemistry and Ecology**
Publication details, including instructions for authors and subscription information:
http://www.informaworld.com/smpp/title~content=t713455114

# Pomegranate husk as an adsorbent in the removal of toxic chromium from wastewater

Ahmed El Nemr[a]
[a] Department of Pollution, Environmental Division, National Institute of Oceanography and Fisheries, Alexandria, Egypt

**To cite this Article** Nemr, Ahmed El(2007) 'Pomegranate husk as an adsorbent in the removal of toxic chromium from wastewater', Chemistry and Ecology, 23: 5, 409 — 425
**To link to this Article: DOI:** 10.1080/02757540701653350
**URL:** http://dx.doi.org/10.1080/02757540701653350

*Chemistry and Ecology*
Vol. 23, No. 5, October 2007, 409–425

Taylor & Francis
Taylor & Francis Group

# Pomegranate husk as an adsorbent in the removal of toxic chromium from wastewater

AHMED EL NEMR*

Department of Pollution, Environmental Division, National Institute of Oceanography and Fisheries, El-Anfoushy, Kayet Bey, Alexandria, Egypt

*(Received 17 April 2007; in final form 21 August 2007)*



The use of a new sorbent developed from the husk of pomegranate, a famous fruit in Egypt, for the removal of toxic chromium from aqueous solution has been investigated. The batch experiment was conducted to determine the adsorption capacity of the pomegranate husk. The effects of initial metal concentration (25 and 50 mg $l^{-1}$), pH, contact time, and sorbent concentration (2–6 g $l^{-1}$) have been studied at room temperature. A strong dependence of the adsorption capacity on pH was observed, the capacity increased as the pH decreased, and the optimum pH value was pH 1.0. Adsorption equilibrium and kinetics were studied with different sorbent and metal concentrations. The adsorption process was fast, and equilibrium was reached within 3 h. The maximum removal was 100% for 25 mg $l^{-1}$ of $Cr^{6+}$ concentration on 5 g $l^{-1}$ pomegranate husk concentration, and the maximum adsorption capacity was 10.59 mg $g^{-1}$. The kinetic data were analysed using various kinetic models—pseudo-first-order, pseudo-second-order, Elovich, and intraparticle diffusion equations—and the equilibrium data were tested using several isotherm models, Langmuir, Freundlich, Tempkin, Dubinin–Radushkevich, and Generalized isotherm equations. The Elovich and pseudo-second-order equations provided the greatest accuracy for the kinetic data, while Langmuir and Generalized isotherm models were the closest fit for the equilibrium data. The activation energy of sorption has also been evaluated as 0.236 and 0.707 kJ $mol^{-1}$ for 25 and 50 mg $l^{-1}$ chromium concentration, respectively.

*Keywords*: Pomegranate husk; Toxic chromium; Kinetics; Isotherm; Adsorption; Wastewater

## 1. Introduction

The contact of industrial pollutants with aquatic ecosystems leads to a risk directly related to the existence of hazardous substances which could have potential negative effects on the biological balance of natural environments. Risk is the probability of appearance of toxic effects after an organism's exposure to hazardous substances. In the context of industrial wastewater discharge into the aquatic ecosystem, exposure to hazardous substances, particularly toxic heavy metals, dyes, non-metabolized pharmaceuticals, hydrocarbons, organochlorines, aromatic amines, and radionuclides requires the consideration of possible risks for aquatic organisms. The fate of pollutants in the aquatic environment has been well documented. The most important regulations from national and international environmental commission fall under the context

*Email: ahmedmoustafaelnemr@yahoo.com

*Chemistry and Ecology*
ISSN 0275-7540 print/ISSN 1029-0370 online © 2007 Taylor & Francis
http://www.tandf.co.uk/journals
DOI: 10.1080/02757540701653350

of risk management concerning human health, and also the management of those concerning the biological balance of natural ecosystems. Ecosystems which may be affected by industrial wastewater are represented by air, soils, surface, and ground water. All biota living in these ecosystems could be affected by exposure to industrial effluents.

Owing to the considerable effects of industrial wastewater on the ecology of the water system, the importance of removing pollutants from industrial wastewater has grown as a consequence of rapid industrialization. Several industries (*i.e.* paint and pigment manufacture, corrosion control, stainless steel production, chrome plating, leather tanning, fertilizers, textile, photography, and wood preservation) discharge effluents containing toxic chromium to surface water. Chromium (Cr) was first discovered in the Siberian red lead ore (crocoite) in 1798 by the French chemist Vauquelin [1]. Chromium is a transition element located in group VI-B of the periodic table with a ground-state electronic configuration of Ar $3d^5 4s^1$. Trivalent and hexavalent species are the stable forms of chromium, while the other valence states are unstable and short-lived in biological systems. Cr(VI) usually occurs associated with oxygen as chromate ($CrO_4^{2-}$) or dichromate ($Cr_2O_7^{2-}$) oxyanions [2]. Hexavalent chromium is considered the most toxic form of chromium, is suspected of being a carcinogen material, and is quite soluble in the aqueous phase almost over the entire pH range in the natural environment. Therefore, as an example, US regulations have set the following limits for chromium discharges: 170 mg $l^{-1}$ of Cr(III) and 0.050 mg $l^{-1}$ of Cr(VI) and USEPA drinking-water regulations limit the total chromium in drinking-water to less than or equal to 0.1 mg $l^{-1}$ [3, 4]. Accidental chromium ingestion causes stomach upsets, ulcers, kidney and liver damage, and even death. Established methods for the removal of chromium oxyanion from wastewater include precipitation, electrochemical reduction, ion exchange, filtration, electrodeposition, membrane technology, reverse osmosis, and adsorption [5]. However, most of these methods have many disadvantages including incomplete metal removal, use of expensive equipment, energy requirements, and production of toxic sludge and other disposal waste products [6–8]. Adsorption remains the most economical and widely used process for removal of toxic pollutants from wastewater. It is by far the most widely used process for the removal of toxic metal ions from aqueous solution. Many reports have appeared on the production of low-cost adsorbents using cheaper and readily available materials [9–16].

The objective of the present study is to evaluate the capacity of a new low-cost adsorbent from pomegranate husk to remove toxic chromium from different aqueous solutions. The batch adsorption process was used to evaluate the maximum adsorption capacity, and several isotherm and kinetic models were used to evaluate the adsorbent. Condition parameters such as pH, contact time, initial metal ion concentrations, and sorbent concentration were considered. The effect of the saline water and wastewater on the adsorption of Cr(VI) was also investigated.

## 2. Materials and methods

### 2.1 *Biomass*

Pomegranate husk (PGH) was collected in the northern part of Egypt and washed with tap water then distilled water, and oven-dried at 105 °C for 3 d. The dried PGH was milled and sieved, and particles $\leq$0.2 mm were selected for investigation.

### 2.2 *Preparation of chromium solution and analysis*

A stock solution of Cr(VI) (1000 mg $l^{-1}$) was obtained by dissolving 2.8289 g of $K_2Cr_2O_7$ salt in 1000 ml of distilled water, and the solution was used for further experimental solution

preparation. Concentrations ranging between 5 and 150 mg $l^{-1}$ were prepared from the stock solution to obtain the standard curve. The pH values were adjusted with 0.1 M HCl or 0.1 M NaOH. All adsorption experiments were carried out at room temperature (25 ± 2 °C), and analytical-grade reagents were used throughout this study. The Cr(VI) content in the sorption medium was determined spectrophotometrically using a double-beam spectrophotometer (Milton Roy, Sectronic 21D). The red-violet-coloured complex of chromium with diphenyl carbazide was read at 540 nm [17, 18].

### 2.3 *Simulation studies*

Synthetic sea water was prepared by dissolving 35 g of NaCl in 1000 ml of distilled water, and the resulting solution was used for the dissolving of $K_2Cr_2O_7$, instead of distilled water used above. Different concentrations of Cr were prepared from the synthetic sea water [11].

Natural sea water was collected from Eastern Harbor, Alexandria, Egypt and filtered using Whatman filter paper. Clear natural sea water was used instead of distilled water to prepare different concentrations of $K_2Cr_2O_7$ [11].

Wastewater was collected from El-Emoum drain located near Lake Maruit, Alexandria, Egypt. This receives several industrial effluents and agriculture drains from the Alexandria Governorate. The collected wastewater was filtered through Whatman filter paper to remove suspended particulates and used to prepare different chromium concentrations [11].



### 2.4 *Batch biosorption studies*

**2.4.1 Effect of pH.** The initial pH values were adjusted to 1.0, 2.1, 3.1, 5.2, 6.3, and 8.2 with 0.1 M HCl or 0.1 M NaOH. The effect of initial pH on the chromium ions adsorption onto PGH was determined at 25 mg $l^{-1}$ initial chromium concentration with 0.5 g/100 ml PGH mass at 25 ± 2 °C for 3 h equilibrium time using an agitation speed of 200 rpm.

**2.4.2 Effect of PGH dose.** The effect of sorbent dose on the removal of Cr(VI) was studied using PGH concentrations of 2, 3, 4, 5, and 6 g $l^{-1}$ by shaking with 25 and 50 mg $l^{-1}$ of Cr concentration for 3 h and was determined from the amount of Cr adsorbed.

**2.4.3 Kinetics studies.** Kinetics studies were achieved at solution pH 1.0 by mixing PGH (0.2, 0.3, 0.4, 0.5, and 0.6 g) with 100 ml of Cr(VI) solution (25 and 50 mg $l^{-1}$) and shaken at room temperature (25 ± 2 °C) for 3 h. Samples of 1.0 ml were collected from the duplicate flasks at different time intervals, centrifuged for 5 min, and the supernatants analysed for residual Cr concentration.

**2.4.4 Adsorption isotherm.** Adsorption isotherm experiments were carried out at room temperature by agitating PGH (0.2, 0.3, 0.4, 0.5, and 0.6 g) with 100 ml of Cr(VI) (25 and 50 mg $l^{-1}$) for 3 h at pH 1.0, and then the reaction mixture was analysed for the residual Cr concentration. All the experiments were duplicated, and only the mean values are reported. The maximum deviation observed was less than 5%.

The amount of Cr(VI) adsorbed onto PGH ($q_e$, mg $g^{-1}$) was calculated using the following equation:

$$q_e = \frac{(C_0 - C_e) \times V}{W}, \tag{1}$$

where $C_0$ and $C_e$ are the initial and equilibrium liquid-phase concentrations (mg $l^{-1}$) of Cr(VI), respectively, $V$ is the volume of the solution (l), and $W$ is the weight of the PGH used (g).

## 3. Results and discussion

### 3.1 *Effect of pH of Cr(VI) solution*

The effect of pH on the adsorption of Cr(VI) by PGH is presented in figure 1. The maximum removal of Cr by PGH was observed at pH 1 and pH 2 as 100% and 95%, respectively. When the initial pH of the solution was increased from 2.0 to 6.3, the percentage removal decreased from 95 to 31%. The maximum adsorption of Cr(VI) occurred at low pH, and this can be attributed to the chromium species and the functional group present in the PGH surface. The $CrO_4^{2-}$ is the predominant species in basic solution, and the predominant species of chromium at acidic pH are $Cr_2O_7^{2-}$, $HCrO_4^-$, $Cr_3O_{10}^{2-}$, and $Cr_4O_{13}^{2-}$ [19–21]. The surface of the PGH became highly protonated under acidic conditions that favoured the adsorption of Cr(VI) in the anionic form. The increase in pH value (towards basic solution) caused a decrease in protonation of the surface, which led to a decrease in the net positive surface potential of sorbent. This decreased the electrostatic forces between sorbent and sorbate, leading to reduced sorption capacity [22]. Moreover, as the pH value increased, there was competition between $OH^-$ and chromate ions.

### 3.2 *Influence of contact time*

Figure 2 shows the percentage removal of Cr(VI) at initial chromium concentrations of 25 and 50 mg $l^{-1}$, respectively, at pH 1.0. The results showed that more than 50% removal of Cr(VI) occurred in the first 30 min, and thereafter the rate of adsorption was rather slow. The removal of Cr(VI) by PGH was 100% and 91% for 25 and 50 mg $l^{-1}$ of initial Cr concentrations, respectively. The rate of Cr binding with PGH was faster in the initial stages and gradually decreased and remained almost constant after 3 h. The slow rate of Cr adsorption after the first 60 min can be attributed to the slow pore diffusion of the Cr ion into the bulk of the PGH.

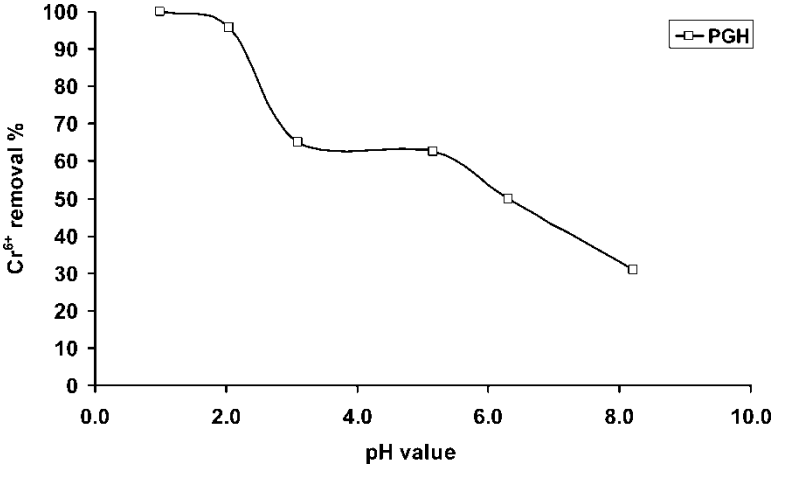


Figure 1. Effect of system pH on adsorption of Cr(VI) (25 mg $l^{-1}$) onto PGH (0.5 g/100 ml) at 25 ± 2 °C.

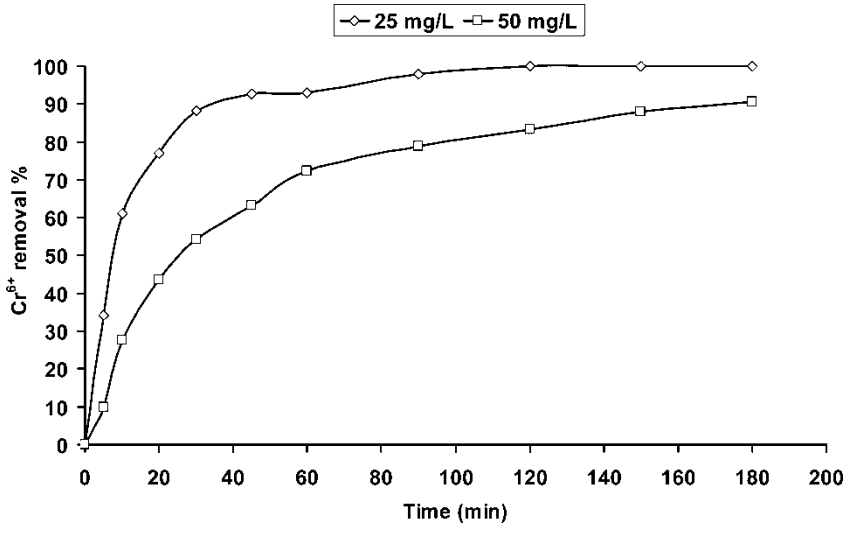


Figure 2. Effect of contact time on the removal of different initial concentrations of Cr(VI) using PGH (0.5 g/100 ml) at pH 1.0.



### 3.3 *Influence of initial chromium concentration and PGH dose*

The adsorption experiments at initial chromium concentrations 25 and 50 mg $l^{-1}$ were also performed with PGH doses (0.2, 0.3, 0.4, 0.5, and 0.6 g/100 ml), and the results are reported in figure 3. Chromium removal decreased, whereas the initial concentration of chromium increased from 25 to 50 mg $l^{-1}$, and this can be explained by the limited number of active sites of the PGH, which would be rapidly saturated. The increasing of the initial metal concentration resulted in a decrease in the initial rate of external diffusion and an increase in the intraparticle diffusion rate.

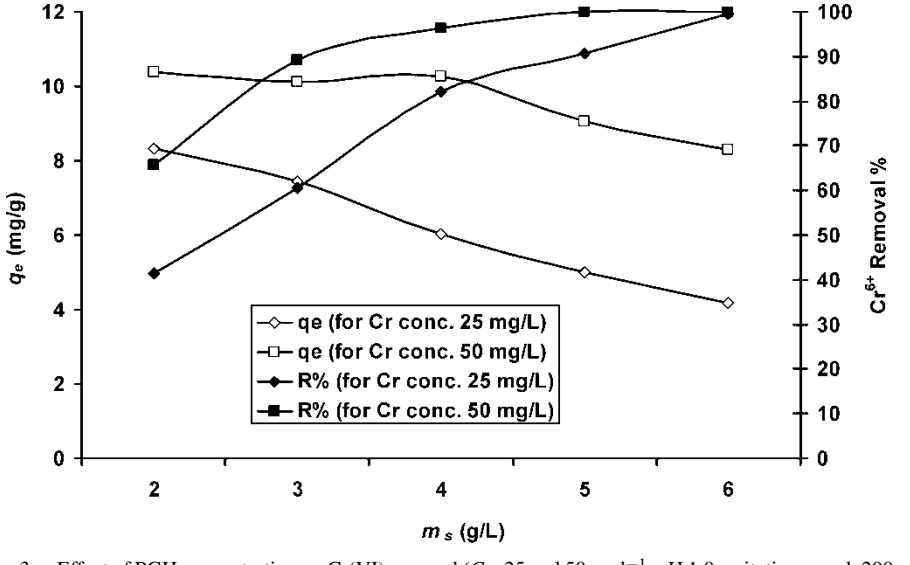


Figure 3. Effect of PGH concentration on Cr(VI) removal ($C_0$: 25 and 50 mg $l^{-1}$, pH 1.0, agitation speed: 200 rpm, temperature: 25 ± 2 °C) and effect of mass ($m_s$) of PGH on $q_e$ of Cr(VI) ($C_0$: 25 and 50 mg $l^{-1}$, pH 1.0, agitation speed: 200 rpm, temperature: 25 ± 2 °C).

The process of metal adsorption first began with the encounter of the metal ions with the boundary layer; then they diffused from the boundary layer film into the PGH surface. Finally, the metal ions diffused into the porous structure of the PGH, and this process took a relatively longer contact time. Figure 3 shows that the amount of Cr adsorbed on PGH at a lower initial concentration of chromium was smaller than the corresponding amount when higher initial concentrations were used. The percentage removal of chromium is higher at lower initial chromium concentrations and vice versa, which clearly indicates that the adsorption of chromium from its aqueous solution was dependent on its initial concentration.

In order to investigate the influence of PGH mass on the amount of chromium adsorption, different PGH masses (from 0.2 to 0.6 g/100 ml using 25 and 50 mg $l^{-1}$ of initial chromium concentrations, respectively) were utilized at room temperature (figure 3). The amount of chromium adsorbed at equilibrium, $q_e$, decreased with increasing PGH mass dose, whereas it increased with increasing initial metal concentration at all investigated PGH doses. The increase in chromium removal with increasing of adsorbent dose can be attributed to the increased surface area and sorption sites, whereas the decrease in adsorption capacity with the increasing of the adsorbent dose can be related to the reduction in effective surface area.



### 3.4 *Adsorption isotherm investigation*

The capacity of an adsorbent can be obtained from the adsorption isotherm that is characterized by certain constant values that express the surface properties and affinity of the adsorbent. The adsorption isotherm models can also be used to compare the adsorptive capacities of the adsorbent for different pollutants. Different isotherm models were used for investigating the equilibrium data to find a suitable model that can be used for the design process. The models used to study the adsorption of chromium by PGH are Langmuir, Freundlich, Tempkin, Dubinin–Radushkevich, and Generalized isotherm equations. The correlation coefficients generally suggest the applicability of isotherm equations.

**3.4.1 Langmuir isotherm.** The most widely used isotherm equation for modelling the equilibrium is the Langmuir equation [23, 24] since it has been used extensively for the adsorption of heavy metals, dyes, organic pollutants, and gases onto activated carbon, clay, and agriculture wastes. The Langmuir equation is valid for monolayer sorption onto a surface of a finite number of identical sites. It assumes uniform energies of adsorption on the surface and no transmigration of sorbate in the plane of the surface [25, 26]. The Langmuir isotherm model suggests an estimation to the maximum adsorption capacity occurred by complete monolayer adsorption on the adsorbent surface. The Langmuir equation can be expressed in the following non-linear form:

$$q_e = \frac{Q_m K_a C_e}{1 + K_a C_e}, \tag{2}$$

where $C_e$ and $q_e$ are defined in equation (1); $K_a$ is adsorption equilibrium constant (l $mg^{-1}$) that is related to the apparent energy of adsorption; and $Q_m$ is the maximum monolayer capacity of the adsorbent (mg $g^{-1}$). Equation (2) can be linearized into the following form [27, 28]:

$$\frac{C_e}{q_e} = \frac{1}{K_a Q_m} + \frac{1}{Q_m} \times C_e. \tag{3}$$

Table 1 shows the results obtained from the linear form of Langmuir equation for the adsorption of Cr(VI) onto PGH. The correlation coefficients for the linear form of Langmuir model are $R^2 = 1.00$, with form 1 being the best fitted for the equilibrium data site $R^2 = 1.000$.

Table 1. Comparison of the coefficients isotherm parameters for chromium adsorption onto PGH.

| Isotherm model | Isotherm parameter | Cr(VI) concentrations | |
|---|---|---|---|
| | | 25 mg l$^{-1}$ | 50 mg l$^{-1}$ |
| Langmuir | $Q_m$ (mg g$^{-1}$) | 8.77 | 10.35 |
| | $K_a \times 10^3$ (l mg$^{-1}$) | 2.23 | 7.32 |
| | $R^2$ | 1.000 | 1.000 |
| Freundlich | $n_F$ | 7.30 | 20.83 |
| | $K_F$ | 6.32 | 8.93 |
| | $R^2$ | 0.977 | 0.951 |
| Tempkin | $A_T$ | 1.19 | $8.84 \times 10^8$ |
| | $B_T$ | 3.38 | 0.43 |
| | $b_T$ | 733 | 5762 |
| | $R^2$ | 0.925 | 0.967 |
| Dubinin–Radushkevich | $Q_m$ | 8.15 | 10.09 |
| | $K \times 10^5$ | 9.00 | 1.00 |
| | $E$ (kJ mol$^{-1}$) | 0.236 | 0.707 |
| | $R^2$ | 0.961 | 0.959 |
| Generalized isotherm | $N_b$ | 0.983 | 0.539 |
| | $K_G$ | 0.439 | 0.115 |
| | $R^2$ | 0.996 | 0.999 |



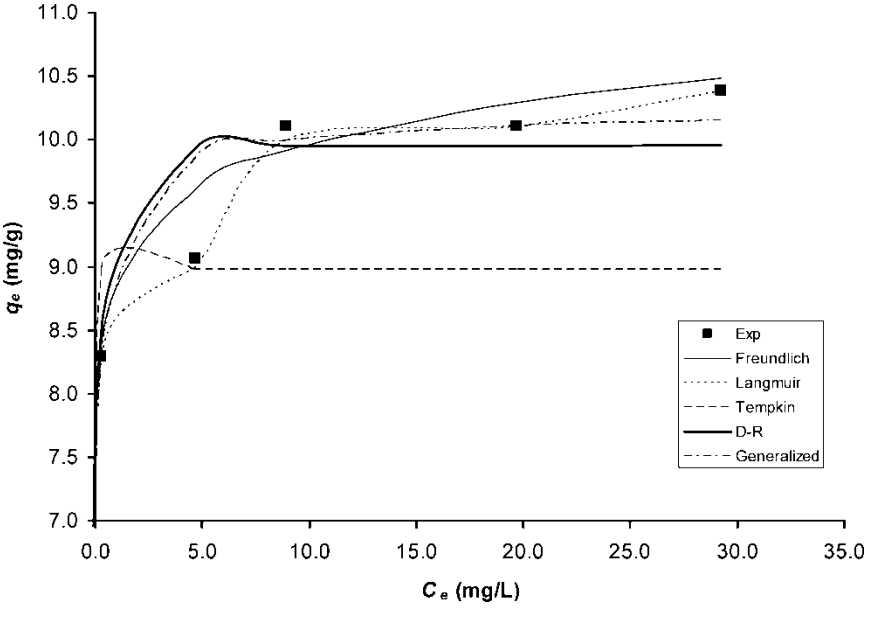


Figure 4. Plot of $C_e$ vs. $q_e$ experimental and calculated using different isotherm models: Langmuir, Freundlich, Tempkin, Dubinin–Radushkevich (D–R) and generalized isotherm models for Cr(VI) (50 mg l$^{-1}$) adsorbed onto PGH (2–6 g l$^{-1}$) at room temperature (25 ± 2 °C).

Figure 4 shows the applicability of the Langmuir isotherm model. The maximum monolayer capacity $Q_m$ obtained from the Langmuir model was 10.6 mg g$^{-1}$, which is comparable with the adsorption capacities of some other adsorbent materials [9].

**3.4.2 Freundlich isotherm.** The first known relationship explaining the adsorption process is the Freundlich isotherm theory [29]. It has been widely adopted to characterize the

adsorption experiments but unfortunately provides no information on the monolayer adsorption capacity, in contrast to the Langmuir model. The Freundlich isotherm equation describes the ratio of the amount of solute adsorbed onto a given mass of sorbent to the concentration of the solute in the solution and is applicable to the adsorption on heterogeneous surfaces with interaction between adsorbed molecules. Therefore, it can be employed to describe the heterogeneous systems and can be expressed as follows:

$$q_e = K_F C_e^{1/n_F}, \tag{4}$$

where $K_F$ is the Freundlich constant (the relative adsorption capacity of the adsorbent related to the bonding energy) and can be defined as the adsorption or distribution coefficient. It represents the quantity of metal adsorbed onto adsorbent for unit equilibrium concentration. The constant $n_F$ is the heterogeneity factor that represents the deviation from linearity of adsorption as follows: (1) $n_F = 1$: the adsorption is linear; (2) $n_F < 1$: the adsorption process is chemical; (3) $n_F > 1$: the adsorption is a favourable physical process [26]. Equation (4) can be linearized via logarithms in the form of equation (5), and the constants can be determined:

$$\log q_e = \log K_F + \frac{1}{n_F} \log C_e. \tag{5}$$

A plot of $\log(q_e)$ vs. $\log(C_e)$ of Freundlich equation and from the obtained figure $K_F$ can be obtained from the intercept value ($\log K_F$ ($\mathrm{mg}^{1-1/n}\,\mathrm{l}^{1/n}\,\mathrm{g}^{-1}$)), and $n_F$ can be estimated from the slope ($1/n_F$; table 1). The correlation coefficients, $R^2 = 0.951$ and 0.977 for 50 and 25 mg $\mathrm{l}^{-1}$ initial chromium concentrations, respectively, showed that the Freundlich model was less applicable than the Langmuir model (figure 4). This indicates that the experimental data fitted well to the Freundlich model, and the $n_F$ values = 7.3 and 20.83 suggest that the adsorption of Cr(VI) onto PGH is a favourable physical process [26].



**3.4.3 Tempkin isotherm.** The adsorbing species–adsorbate interactions can be explained using the Tempkin isotherm equation [30]. It is based on the assumption that the heat of adsorption of all the molecules in the layer decreases linearly with coverage due to adsorbate–adsorbate repulsions, and the adsorption is a uniform distribution of maximum binding energy [31]. In addition, it assumes that the fall in the heat of sorption is linear rather than logarithmic, as implied in the Freundlich equation. It is commonly expressed in the following equation (6) [32–34]:

$$q_e = \frac{RT}{b_T} \ln(A_T C_e) \quad \text{(non-linear form)} \tag{6}$$

$$q_e = B_T \ln A_T + B_T \ln C_e, \quad \text{(linear form)} \tag{7}$$

where $B_T = (RT)/b_T$, $T$ is the absolute temperature (K), and $R$ is the universal gas constant, 8.314 J $\mathrm{mol}^{-1}$ $\mathrm{K}^{-1}$. The constant $b_T$ is related to the heat of adsorption; $A_T$ is the equilibrium binding constant (l $\mathrm{min}^{-1}$) corresponding to the maximum binding energy [35, 36]. The adsorption data can be analysed according to equation (7) from a plot of $q_e$ vs. ln $C_e$ followed by determination of the isotherm constants $A_T$ and $b_T$ and correlation coefficients (table 1). The correlation coefficients are 0.925 and 0.967 for 25 and 50 mg $\mathrm{l}^{-1}$ chromium concentrations, respectively. These values suggest that the Tempkin isotherm is less applicable than the Langmuir and Freundlich models. This can be clearly observed in the figure 4, when the calculated $q_e$ values are not similar to those obtained from the experimental work.

**3.4.4 Dubinin–Radushkevich isotherm.** The Dubinin–Radushkevich (D–R) model [37] is another equation used in the analysis of isotherms. While it does not assume a homogeneous surface or constant sorption potential, this model is applied to estimate the porosity apparent free energy and the characteristics of adsorption. It has commonly been applied in the following forms [38–40]:

$$q_e = Q_m \exp(-K\varepsilon^2) \quad \text{(non-linear form)} \tag{8}$$

$$\ln q_e = \ln Q_m - K\varepsilon^2 \quad \text{(linear form)}, \tag{9}$$

where $K$ is a constant related to the adsorption energy and $Q_m$ the maximum adsorption capacity. $\varepsilon$ can be calculated from equation (10):

$$\varepsilon = RT \ln\left(1 + \frac{1}{C_e}\right), \tag{10}$$

The plot of $\ln q_e$ vs. $\varepsilon^2$ for the experimental data for the adsorption of Cr(VI) by PGH gave the constants $K$ (mol$^2$ (kJ$^2$)$^{-1}$) and $Q_m$ (mg g$^{-1}$) by calculation from the slope and the intercept, respectively (table 1). The mean free energy of adsorption ($E$) is the free energy change when 1 mol of ion transferred from infinity in solution to the surface of the sorbent. $E$ is calculated from the $K$ value using equation (11) [41]:

$$E = \frac{1}{\sqrt{(2K)}}. \tag{11}$$

The correlation coefficients values were 0.961 and 0.959 for 25 and 50 mg l$^{-1}$ chromium concentrations, respectively, and suggested that the D–R model also fitted the experimental data less well in comparison with the Langmuir and Freundlich models. However, the maximum capacity, $Q_m$, obtained from the D–R isotherm model for adsorption of Cr(VI), is comparable with that obtained from the Langmuir model. This finding may be explained by the applicability of the D–R isotherm model to the adsorption of chromium into PGH, since the calculated $q_e$ from D–R isotherm is comparable with that obtained from the experimental work (figure 4).



**3.4.5 Generalized isotherm equation.** A generalized isotherm equation was tested for correlation of the equilibrium data [42–44]. The linear form of the generalized isotherm is:

$$\log\left[\frac{Q_m}{q_e} - 1\right] = \log K_G - N_b \log C_e, \tag{12}$$

where, $K_G$ is the saturation constant (mg l$^{-1}$); $N_b$ the cooperative binding constant; $Q_m$ the maximum adsorption capacity of the adsorbent (mg g$^{-1}$) (obtained from Langmuir isotherm model); $q_e$ (mg g$^{-1}$) and $C_e$ (mg l$^{-1}$) are the equilibrium chromium concentrations in the solid and liquid phases, respectively. Plot of $\log[(Q_m/q_e) - 1]$ vs. $\log C_e$; the intercept gave $\log K_G$, and the slope gave $N_b$ constants. Parameters related to each isotherm were determined by using linear regression analysis, and the square of the correlation coefficients ($R^2$) was calculated (table 1). Apparently, the generalized adsorption isotherm represents the equilibrium data reasonably well (figure 4). The exponent ($K_G$) was 0.439 and 0.115 for 25 and 50 mg l$^{-1}$ chromium concentrations, respectively, which reflects the fact that the generalized isotherm approximates to the Langmuir expression. The data reported in tables 2 and 3 showed that most of the isotherm models tested are in accordance with the experimental data obtained for the adsorption of Cr(VI) on PGH.

Table 2. Comparison of the first- and second-order adsorption rate constants and calculated and experimental $q_e$ values for different initial chromium and PGH concentrations.

| Parameter | | | First-order kinetic model | | | Second-order kinetic model | | | |
|---|---|---|---|---|---|---|---|---|---|
| PGH conc. ($g\,l^{-1}$) | Cr(VI) ($mg\,l^{-1}$) | $q_e$ (exp.) | $k_1 \times 10^3$ | $q_e$ (calc.) | $R^2$ | $k_2 \times 10^3$ | $q_e$ (calc.) | $h$ ($mg\,g^{-1}\,min^{-1}$) | $R^2$ |
| 2.0 | 25 | 8.33 | 14.97 | 8.71 | 0.990 | 2.44 | 8.44 | 0.17 | 0.998 |
| | 50 | 10.38 | 8.29 | 8.32 | 0.852 | 1.80 | 10.20 | 0.19 | 0.995 |
| 3.0 | 25 | 7.43 | 21.65 | 6.82 | 0.980 | 3.00 | 8.99 | 0.24 | 0.998 |
| | 50 | 10.11 | 19.35 | 10.39 | 0.957 | 1.86 | 10.40 | 0.20 | 0.999 |
| 4.0 | 25 | 6.02 | 28.79 | 5.14 | 0.980 | 7.93 | 6.68 | 0.35 | 0.998 |
| | 50 | 10.06 | 17.96 | 7.84 | 0.985 | 3.01 | 10.17 | 0.31 | 0.998 |
| 5.0 | 25 | 5.00 | 37.08 | 2.66 | 0.939 | 26.16 | 5.25 | 0.72 | 1.000 |
| | 50 | 9.07 | 21.65 | 7.68 | 0.985 | 3.84 | 9.33 | 0.33 | 0.999 |
| 6.0 | 25 | 4.17 | 49.05 | 2.28 | 0.912 | 47.13 | 4.31 | 0.87 | 1.000 |
| | 50 | 8.29 | 23.72 | 5.66 | 0.986 | 7.25 | 8.56 | 0.53 | 1.000 |

Table 3. Parameters obtained from Elovich kinetics model and intraparticle diffusion model using different initial Cr(VI) concentrations and PGH doses.

| | | Elovich | | | Intraparticle diffusion | | |
|---|---|---|---|---|---|---|---|
| PGH dose ($g\,l^{-1}$) | Cr(VI) conc. | $\beta$ | $\alpha$ | $R^2$ | $K_{dif}$ | $B_L$ | $R^2$ |
| 2.0 | 25 | 0.33 | 0.25 | 0.995 | 0.62 | 0.05 | 0.993 |
| | 50 | 0.56 | 0.93 | 0.987 | 0.80 | 0.24 | 0.965 |
| 3.0 | 25 | 0.51 | 0.54 | 0.994 | 0.52 | 1.02 | 0.938 |
| | 50 | 0.33 | 0.48 | 0.998 | 0.72 | 0.76 | 0.991 |
| 4.0 | 25 | 0.72 | 0.82 | 0.995 | 0.36 | 1.77 | 0.915 |
| | 50 | 0.44 | 1.10 | 0.994 | 0.65 | 2.13 | 0.965 |
| 5.0 | 25 | 1.17 | 3.40 | 0.986 | 0.16 | 3.20 | 0.743 |
| | 50 | 0.44 | 0.77 | 0.995 | 0.53 | 2.45 | 0.955 |
| 6.0 | 25 | 1.34 | 2.77 | 0.991 | 0.11 | 3.93 | 0.611 |
| | 50 | 0.60 | 1.71 | 0.992 | 0.42 | 3.23 | 0.892 |

### 3.5 *Adsorption kinetic considerations*



The dynamics of the adsorption reaction in terms of the order of the rate constant can be understood by studying the kinetic of the adsorption. Batch experiments were conducted to study the rate of Cr (25 and 50 $mg\,l^{-1}$) adsorption by PGH (2–6 $g\,l^{-1}$) at pH 1. Several models were studied to examine the rate-controlling steps of the adsorption process such as chemical reaction, diffusion control and mass transfer. The pseudo-first-order [45], pseudo-second-order [46], Elovich [47–49], and intraparticle diffusion [50, 51] kinetic models were used for the adsorption of Cr on PGH, and their applicability was expressed by the correlation coefficients ($R^2$).

**3.5.1 Pseudo first-order equation.** The earliest known equation describing the adsorption rate based on the adsorption capacity is Lagergren's pseudo-first-order model [45], which is commonly expressed as follows:

$$\frac{dq_t}{dt} = k_1(q_e - q_t), \tag{13}$$

where, $q_e$ and $q_t$ refer to the amount of Cr adsorbed ($mg\,g^{-1}$) at equilibrium and at any time, $t$ (min), respectively, and $k_1$ is the equilibrium rate constant of pseudo-first-order adsorption ($l\,min^{-1}$). Integrating equation (13) for the boundary conditions $t = 0$ to $t$ and $q_t = 0$ to $q_t$ gives:

$$\log\left(\frac{q_e}{q_e - q_t}\right) = \frac{k_1}{2.303}t, \tag{14}$$

which is the integrated rate law for a pseudo-first-order reaction. Equation (14) can be rearranged to obtain the linear form:

$$\log(q_e - q_t) = \log(q_e) - \frac{k_1}{2.303}t. \tag{15}$$

Values of the rate constant, $k_1$, equilibrium adsorption capacity, $q_e$, and the correlation coefficient, $R^2$, were calculated from the plots of $\log(q_e - q_t)$ vs. $t$. Although the correlation coefficients obtained from the pseudo-first-order model are found to be mainly high, the calculated $q_e$ values do not agree with experimental values (table 2, figure 5). This indicates that adsorption of Cr onto PGH is not an ideal pseudo-first-order reaction [26].

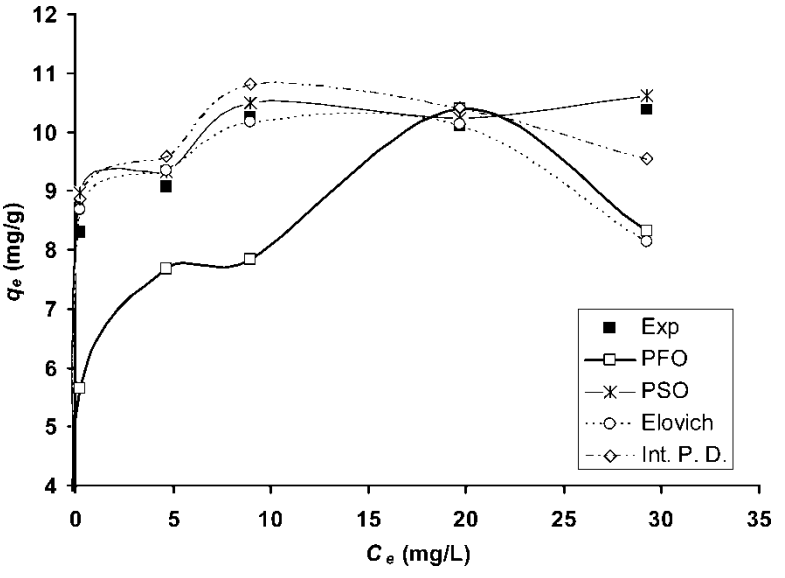


Figure 5. Plot of $C_e$ vs. $q_e$ experimental and calculated for pseudo-first-order (PFO) kinetics, pseudo-second-order (PSO), Elovich model, and Intraparticle diffusion (Int. P. D.) model for the adsorption of Cr(VI) onto PGH (2–6 g $l^{-1}$) at initial Cr concentration (50 mg $l^{-1}$), pH 1.0, and room temperature (25 ± 2 °C).



**3.5.2 Pseudo second-order equation.** The pseudo-second-order kinetic model was further applied to the kinetic data [46]. The equation is commonly expressed as follows:

$$\frac{dq_t}{dt} = k_2(q_e - q_t)^2, \tag{16}$$

where $k_2$ (g/mg min) is the equilibrium rate constant of pseudo-second-order adsorption. Integrating equation (16) for the boundary conditions $q_t = 0$ to $q_t$ and $t = 0$ to $t$ gives:

$$\left(\frac{t}{q_t}\right) = \frac{1}{k_2 q_e^2} + \frac{1}{q_e}(t). \tag{17}$$

The initial adsorption rate, $h$ (mg $g^{-1}$ $min^{-1}$) is expressed by the following equation (18):

$$h = k_2 q_e^2. \tag{18}$$

If the plots of $t/q_t$ vs. $t$ show a linear relationship, the pseudo-second-order kinetics will become applicable. The linear plot $t/q_t$ vs. $t$ shows a good agreement for the experimental data with the pseudo-second-order kinetic model for adsorption of Cr on PGH. The correlation coefficients ($R^2$) for the second-order kinetics model are higher than 0.99. The second-order rate constant, $k_2$, and the equilibrium adsorption capacity, $q_e$, were calculated from the intercept and slope of the plots of $t/q_t$ vs. $t$. The calculated $q_e$ values agree very well with the experimental data (table 2, figure 5). These suggest that the adsorption of Cr from aqueous solution on PGH follows the pseudo-second-order model.

The pseudo-second-order rate constant ($k_2$) decreased with increasing initial chromium concentration from 25 to 50 mg $l^{-1}$ (table 2), while the values of initial adsorption rate ($h$), the rate of initial adsorption, practically increased with increasing initial chromium concentrations (figure 6).

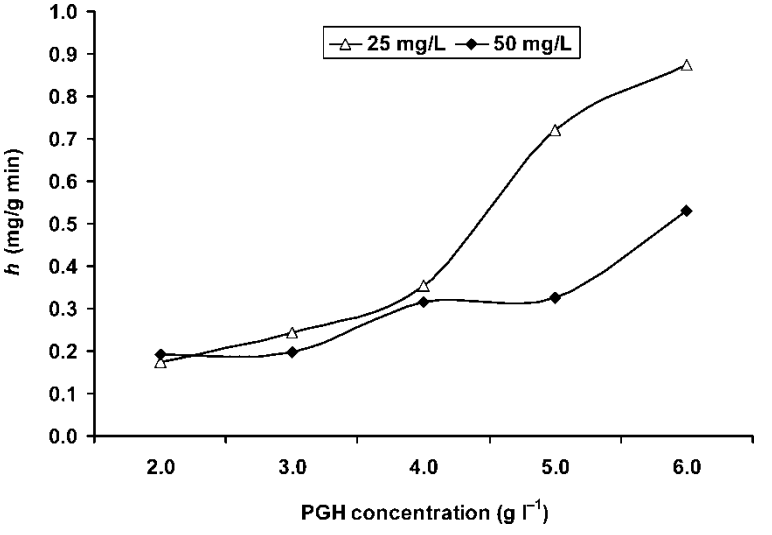


Figure 6. Plot of $h$ of the pseudo-second-order model at different initial Cr(VI) concentrations, PGH 2.0–6.0 g l$^{-1}$, pH 1.0, temperature 25 ± 2 °C.



**3.5.3 Elovich kinetic equation.** Elovich equation is a rate equation based on the adsorption capacity commonly expressed as the following equation (19) [47–49]:

$$\frac{\mathrm{d}q_t}{\mathrm{d}t} = \alpha \exp(-\beta q_t), \tag{19}$$

where $\alpha$ is the initial adsorption rate (mg g$^{-1}$ min$^{-1}$), and $\beta$ is the desorption constant (g mg$^{-1}$) related to the extent of surface coverage and activation energy for chemisorptions. Equation (19) is simplified by assuming $\alpha\beta \gg t$ and by applying the boundary conditions $q_t = 0$ at $t = 0$, and $q_t = q_t$ at $t = t$ becomes:

$$q_t = \frac{1}{\beta}\ln(\alpha\beta) + \frac{1}{\beta}\ln(t). \tag{20}$$

Plots of $q_t$ vs. $\ln(t)$ and the Elovich constants $\alpha$ and $\beta$ were calculated from the intercept and slope, respectively (table 3). The correlation coefficients, $R^2 > 0.98$, are comparable with correlation coefficients obtained for the pseudo-second-order model, which reflected the applicability of the Elovich model to the adsorption of Cr on PGH (figure 5).

**3.5.4 Intraparticle diffusion model.** Adsorption of any metal ions from its solution onto any solid sorbent is a multi-step process starting with: (1) bulk diffusion defined as transport of metal ions from solution to the surface of the solid particles; (2) film diffusion defined as diffusion of metal ions via the boundary layer to the surface of the solid particles; and (3) pore diffusion or intraparticle diffusion defined as transport of metal ions from the solid particle surface to its interior pores. The third process is likely to be a slow process and may be the rate-determining step. In addition, adsorption of metal ions at an active site on the solid phase surface could also have occurred by chemical reaction such as ion-exchange, complexation, and chelation. Metal-ion adsorption is usually controlled by either the intraparticle (pore diffusion) or the liquid-phase mass transport rates [26]. If the experiment is a batch system with rapid stirring, there is a possibility that intraparticle diffusion is the rate-determining step

[52]. Weber and Morris [50] provided the rate for intraparticle diffusion by the relationship between $q_t$ and the square root of time, $t^{1/2}$, as shown in equation (21):

$$q_t = K_{\text{dif}} t^{1/2} + B_{\text{L}}, \tag{21}$$

where $B_{\text{L}}$ is related to the thickness of the boundary layer, and $K_{\text{dif}}$ (mg g$^{-1}$ min$^{-1/2}$) is the intraparticle diffusion rate constant. $K_{\text{dif}}$ and $B_{\text{L}}$ values are calculated from the slope and intercept of $q_t$ vs. $t^{1/2}$ plots, respectively.

The intraparticle diffusion is another kinetic model to study the rate-determining step for Cr adsorption onto PGH. A plot of $q_t$ vs. $t^{1/2}$ for adsorption of Cr (25 and 50 mg l$^{-1}$) on PGH (2.0 g l$^{-1}$) and the values of $K_{\text{dif}}$ and $B_{\text{L}}$ are reported in table 3.

If the plot of $q_t$ vs. $t^{1/2}$ gave a linear relationship, the intraparticle diffusion would be involved in the adsorption process, and it would be the controlling step if this line passed through the origin [26]. The shape of plot of $q_t$ vs. $t^{1/2}$ (figure 7) confirms that straight lines did not pass through the origin for all PGH concentrations studied. The correlation coefficients ranged between 0.611 and 0.993. The results obtained from intraparticle diffusion model indicate that there are some degrees of boundary layer for the higher PGH concentrations, which indicates that the intraparticle diffusion is not only the rate-controlling step for the adsorption of the Cr on PGH (figure 5).

On the other hand, figure 8 shows the plot between $C$ and $K_{\text{dif}}$ vs. PGH concentrations. The $B_{\text{L}}$ value was found to increase with increasing PGH concentration, which suggested an increase in the thickness of the boundary layer and a decrease in the chance of external mass transfer (hence the chance of internal mass transfer). The intraparticle diffusion rate constant, $K_{\text{dif}}$, decreased with decreasing initial chromium concentration and increasing PGH concentration (table 3).



### 3.6 *Applicability on real wastewater and saline water*

The applicability of chromium removal on PGH was tested using artificial and natural sea water and real wastewater. The percentage of chromium removal by PGH from aqueous

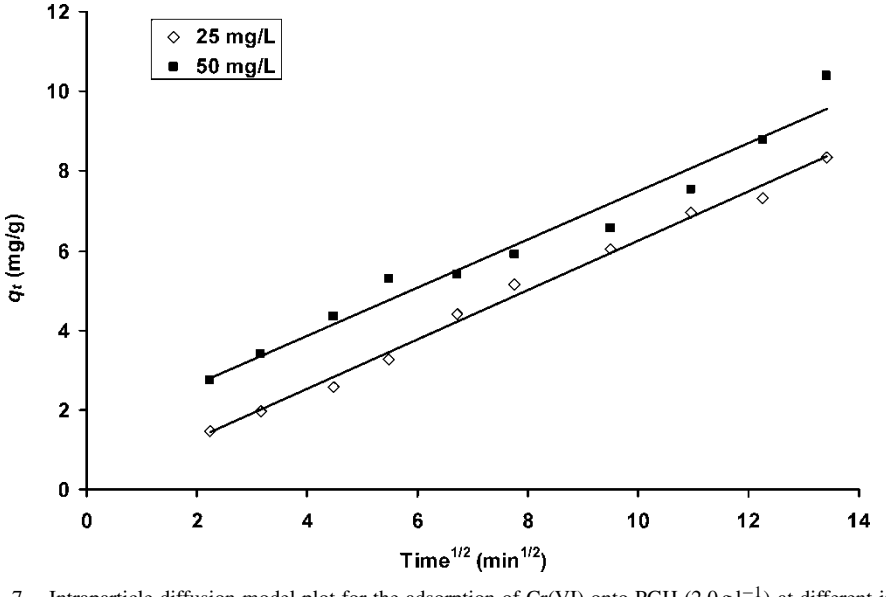


Figure 7. Intraparticle diffusion model plot for the adsorption of Cr(VI) onto PGH (2.0 g l$^{-1}$) at different initial Cr concentrations (25 and 50 mg l$^{-1}$) and room temperature.

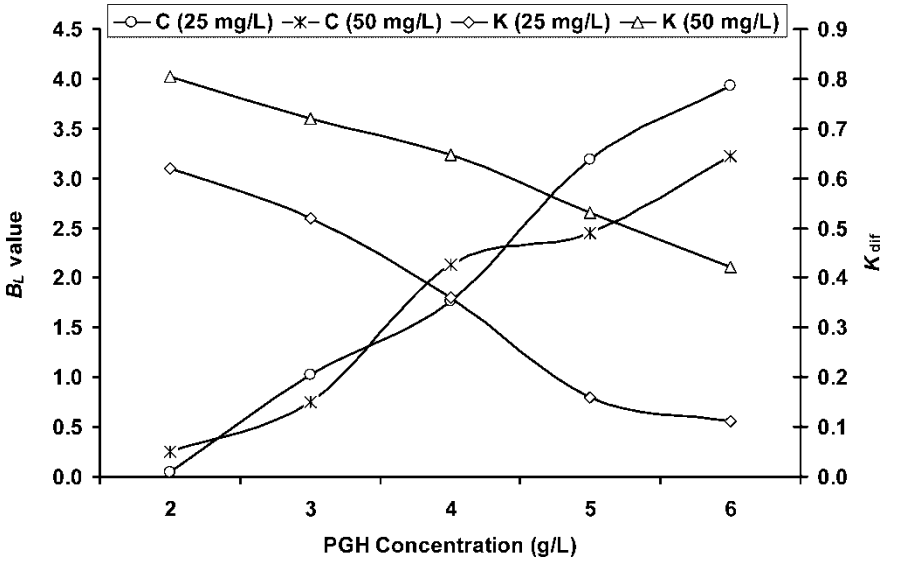


Figure 8. Plot of PGH concentrations (2.0–6.0 mg $l^{-1}$) vs. intraparticle diffusion constant $B_L$ and $K_{dif}$ values obtained for different PGH doses at room temperature.

Table 4. Data obtained for the adsorption of Cr(VI) (25 mg $l^{-1}$) from different solutions using PGH (5.0 g $l^{-1}$).

| | PGH | |
|---|---|---|
| Solution of chromium used | Removal % | Maximum capacity (mg $g^{-1}$) |
| Distilled water | 100.00 | 10.48 |
| Artificial sea water | 98.12 | 10.22 |
| Natural sea water | 97.25 | 10.08 |
| Wastewater | 98.84 | 10.29 |

solution was not affected by replacing distilled water with artificial sea water, natural sea water, or wastewater (table 4). Almost 98% removal of toxic chromium from synthetic sea water, natural sea water, and wastewater was detected for PGH. Moreover, the maximum adsorption capacities were not significantly changed by changing the type of chromium solution. The presence of salt had no effect on the removal of chromium by PGH, suggesting that there was no interaction between the salt and the PGH or the salt and the Cr. In real wastewater, the higher concentration of chromium ions than the other pollutants may make Cr ions more preferable for adsorbtion by PGH. On the other hand, the real wastewater may contain very low concentrations from several pollutants that will have little effect on the removal efficiency of chromium ions. These results indicate that the newly developed PGH is an applicable material for removal of Cr(VI) ions from different types of aqueous solutions, including wastewater.

## 4. Conclusion

This study suggests that PGH is an effective adsorbent for the removal of toxic chromium from its aqueous solution. The excess positive charge on the PGH surface enables the adsorption of toxic chromium (VI) ions. The first-order and second-order kinetic models suggest that the adsorption process preferably obeys the second-order kinetic models, which provides a

higher correlation coefficient and calculated $q_e$ results comparable with the experimental $q_e$. However, the adsorption of chromium on PGH is a complex process and cannot be adequately described by a single kinetic model throughout the whole process. The Elovich and intraparticle diffusion models suggest that the intraparticle diffusion played a significant role, but it was not the main rate-determining step during the adsorption process. The Langmuir, Freundlich, and Generalized isotherm models fit the experimental data reasonably well, while the Tempkin and Dubinin–Radushkevich isotherm models are not applicable. The PGH exhibits a maximum adsorption capacity of 10.6 mg $l^{-1}$. The percentage removal and maximum adsorption capacity are not affected by sodium chloride ions in the solution or by replacing the distilled water by natural sea water or real wastewater. Since the raw material PGH is freely available in large quantities as a waste from the juice industries, the treatment method would seem to be economical. Based on the above results, this relatively low-cost PGH is recommended as an effective and cheap adsorbent for removal of chromium from textile effluents. Since the ecotoxicological risk of Cr(VI) has been well documented, as mentioned in section 1, removal of toxic Cr(VI) from wastewater using natural material such as PGH will certainly have a positive effect on the ecosystems.



## References


[1] A.K. Shanker, C. Cervantes, H. Loza-Tavera, S. Avudainayagam. Chromium toxicity in plants. *Environ. Int.*, **31**, 739 (2005).

[2] F. Gode, E. Pehlivan. Removal of Cr(VI) from aqueous solution by two Lewatit-anion exchange resins. *J. Hazard. Mater.*, **B119**, 175 (2005).

[3] EPA. USEPA Report no. EPA/570/9–76/003; Washington, DC (1976).

[4] R.R. Patterson, S. Fendorf, M. Fendorf. Reduction of hexavalent chromium by amorpous iron sulfide. *Environ. Sci. Technol.*, **31**, 2039 (1997).

[5] G. Rich, K. Cherry. *Cited in Hazardous Waste Treatment Technology*, Pudvan, New York (1987).

[6] B. Volesky. *Biosorption of Heavy Metals*, CRC Press, Boston (1990).

[7] M.C. Basso, E.G. Cerrella, A.L. Cukierman. Empleo de algas marinas para la biosorción de metales pesados de aguas contaminadas. *Avances en Energías Renovables Medio Ambiente*, **6**, 59 (2002).

[8] Z. Aksu, F. Gönen, Z. Demircan. Biosorption of chromium(VI) ions by Mowital B3OH resin immobilized activated sludge in a packed bed: comparison with granular activated carbon. *Process. Biochem.*, **38**, 175 (2002).

[9] S. Babel, T.A. Kurniawan. Low-cost adsorbents for heavy metals uptake from contaminated water: a review. *J. Hazard. Mater.*, **B97**, 219 (2003).

[10] A. Baran, Biçak, Ş.H. Baysal, S. Önal. Comparative studies on the adsorption of Cr(VI) ions on to various sorbents. *Bioresour. Technol.*, **98**, 661 (2006).

[11] A. El-Sikaily, A. El Nemr, A. Khaled, O. Abdelwahab. Removal of toxic Chromium from wastewater using green alga *Ulva lactuca* and its activated Carbon. *J. Hazard. Mater.*, **148**(1–2), 216 (2007).

[12] O. Abdelwahab, A. El Nemr, A. El-Sikaily, A. Khaled. Biosorption of Direct Yellow 12 from aqueous solution by marine green algae *Ulva lactuca*, *Chem. Ecology*, **22**(4), 253 (2006).

[13] A. El-Sikaily, A. Khaled, A. El Nemr, O. Abdelwahab. Removal of methylene blue from aqueous solution by marine green alga *Ulva lactuca*. *Chem. Ecology*, **22**(2), 149 (2006).

[14] A. El Nemr, A. El-Sikaily, A. Khaled, O. Abdelwahab. Removal of toxic chromium(VI) from aqueous solution by activated carbon using *Casuarina Equisetifolia*. *Chem. Ecology*, **23**(2), 119 (2007).

[15] O. Abdelwahab, A. El-Sikaily, A. Khaled, A. El Nemr. Mass transfer processes of chromium(VI) adsorption onto Guava seeds. *Chem. Ecol.*, **23**(1), 73 (2007).

[16] S. Mor, K. Ravindra, N.R. Bishnoi. Adsorption of chromium from aqueous solution by activated alumina and activated charcoal. *Bioresour. Technol.*, **98**, 954 (2007).

[17] F.D. Snell, C.T. Snell. *Colorimetric Methods of Analysis*, 3rd ed., InterScience, New York (1961).

[18] F.W. Gilcreas, M.J. Tarars, R.S. Ingols. *Standard Methods for the Examination of water and wastewater*, 12th ed., American Public Health Association, New York (1965).

[19] C. Raji, T.S. Anirudhan. Batch Cr(VI) removal by polyacrylamide-grafted sawdust: kinetics and thermodynamics. *Water Res.*, **32**(10), 3772 (1998).

[20] B.M. Weckhuysen, I.E. Wachs, R.A. Schoonheydt. Surface chemistry and spectroscopy of chromium in inorganic oxides. *Chem. Rev.*, **96**, 3327 (1996).

[21] S. Mor, K. Ravindra, N.R. Bishnoi. Adsorption of chromium from aqueous solution by activated alumina and activated charcoal. *Bioresour. Technol.*, **98**, 954 (2007).

[22] K. Selvi, S. Pattabhi, K. Kadirvelu. Removal of Cr(VI) from aqueous solution by adsorption onto activated carbon. *Bioresour. Technol.*, **80**, 87 (2001).

[23] I. Langmuir. The constitution and fundamental properties of solids and liquids. *J. Am. Chem. Soc.*, **38**, 2221 (1916).
[24] I. Langmuir. The adsorption of gases on plane surfaces of glass, mica and platinum. *J. Am. Chem. Soc.*, **40**, 1361 (1918).
[25] M. Doğan, M. Alkan, Y. Onganer. Adsorption of methylene blue from aqueous solution onto perlite. *Water Air Soil Pollut.*, **120**, 229 (2000).
[26] G. Crini, H.N. Peindy, F. Gimbert, C. Robert. Removal of C.I. Basic Green 4 (Malachite Green) from aqueous solutions by adsorption using cyclodextrin-based adsorbent: Kinetic and equilibrium studies. *Sep. Purif. Technol.*, **53**, 97 (2007).
[27] D.G. Kinniburgh. General purpose adsorption isotherms. *Environ. Sci. Technol.*, **20**, 895 (1986).
[28] E. Longhinotti, F. Pozza, L. Furlan, M.D.N.D. Sanchez, M. Klug, M.C.M. Laranjeira, V.T. Favere. Adsorption of anionic dyes on the biopolymer chitin. *J. Brazil. Chem. Soc.*, **9**, 435 (1998).
[29] H.M.F. Freundlic. Über die adsorption in lösungen. *Zeitschrift für Physikalische Chemie (Leipzig)*, **57A**, 385 (1906).
[30] M.J. Tempkin, V. Pyzhev. *Acta Physiochim, URSS*, **12**, 217 (1940).
[31] D. Kavitha, C. Namasivayam. Experimental and kinetic studies on methylene blue adsorption by coir pith carbon. *Bioresour. Technol.*, **98**, 14 (2007).
[32] C. Aharoni, D.L. Sparks. Kinetics of Soil Chemical Reactions—A Theoretical Treatment. In D.L. Sparks and D.L. Suarez (Eds), *Rate of Soil Chemical Processes*, Soil Science Society of America, Madison, WI, pp. 1–18 (1991).
[33] C. Aharoni, M. Ungarish, Kinetics of activated chemisorption. Part 2. Theoretical models. *J. Chem. Soc., Faraday Trans.*, **73**, 456 (1977).
[34] X.S. Wang, Y. Qin. Equilibrium sorption isotherms for of Cu(II) on rice bran. *Proc. Biochem.*, **40**, 677 (2005).
[35] C.I. Pearce, J.R. Lioyd, J.T. Guthrie. The removal of color from textile wastewater using whole bacterial cells: a review. *Dyes Pigments*, **58**, 179 (2003).
[36] G. Akkaya, A. Ozer. Adsorption of acid red 274 (AR 274) on *Dicranella varia*: determination of equilibrium and kinetic model parameters. *Proc. Biochem.*, **40**(9), 3559 (2005).
[37] M.M. Dubinin, L.V. Radushkevich. Equation of the characteristic curve of activated charcoal. *Chem. Zentr.*, **1**, 875 (1947).
[38] L.V. Radushkevich. Potential theory of sorption and structure of carbons. *Zhurnal Fizicheskoi Khimii*, **23**, 1410 (1949).
[39] M.M. Dubinin. The potential theory of adsorption of gases and vapors for adsorbents with energetically nonuniform surface. *Chem. Rev.*, **60**, 235 (1960).
[40] M.M. Dubinin. Modern state of the theory of volume filling of micropore adsorbents during adsorption of gases and steams on carbon adsorbents. *Zhurnal Fizicheskoi Khimii*, **39**, 1305 (1965).
[41] S. Kundu, A.K. Gupta. Investigation on the adsorption efficiency of iron oxide coated cement (IOCC) towards As (V)-Kinetics, equilibrium and thermodynamic studies. *Colloids Surf. A: Physicochem. Eng. Aspects*, **273**, 121 (2006).
[42] F. Kargi, S. Ozmichi. Biosorption performance of powdered activated sludge for removal of different dyestuffs. *Enzyme Microb. Technol.*, **35**, 267 (2004).
[43] S. Ozmihci, F. Kargi. Utilization of powdered waste sludge (PWS) for removal of textile dyestuffs from wastewater by adsorption. *J. Environ. Managem.*, **81**, 307 (2006).
[44] F. Kargi, S. Cikla, Biosorption of zinc(II) ions onto powdered waste sludge (PWS): kinetics and isotherms. *Enzyme Microb. Technol.*, **38**, 705 (2006).
[45] S. Lagergren. Zur theorie der sogenannten adsorption geloster stoffe. *Kungliga Svenska Vetenskapsakademiens. Handlingar*, **24**, 1 (1898).
[46] Y.S. Ho, G. McKay, D.A.J. Wase, C.F. Foster. Study of the sorption of divalent metal ions on to peat. *Adsorp. Sci. Technol.*, **18**, 639 (2000).
[47] Zeldowitsch J. Über den mechanismus der katalytischen oxidation von CO and $MnO_2$. *Acta Physicochim. URSS*, **1**, 364 (1934).
[48] S.H. Chien, W.R. Clayton. Application of Elovich equation to the kinetics of phosphate release and sorption on soils. *Soil. Sci. Soc. Am. J.*, **44**, 265 (1980).
[49] D.L. Sparks. Kinetics of reaction in pure and mixed systems. In *Soil Physical Chemistry*, CRC Press, Boca Raton, FL, 85 (1986).
[50] W.J. Weber, J.C. Morris. Kinetics of adsorption on carbon from solution. *J. Sanity Eng. Div. Am. Soc. Civil Eng.*, **89**, 31 (1963).
[51] K. Srinivasan, N. Balasubramanian, T.V. Ramakrishan. Studies on chromium removal by rice husk carbon. *Indian J. Environ. Health*, **30**, 376 (1988).
[52] G. McKay. The adsorption of dyestuff from aqueous solution using activated carbon: analytical solution for batch adsorption based on external mass transfer and pore diffusion. *Chem. Eng. J.*, **27**, 187 (1983).